

# Fast and Accurate Determination of the Complex Resonant Frequency of a Multilayer Circular Cavity Using Chebyshev's Root-finder

David Marques-Villarroya<sup>\*</sup>, Felipe L. Penaranda-Foix, Beatriz Garcia-Banos, Jose M. Catala-Civera, and Jose D. Gutierrez-Cano

**Abstract**—In this paper, a general multilayer circular cavity with  $N$  slabs is analyzed analytically, obtaining characteristic equations for TE and TM modes to compute the complex resonant frequency efficiently using an algorithm based on Chebyshev's root finder. The accuracy of the solutions is compared with *full-wave circuit* method, and the computational speed to achieve the roots of the characteristic equations is also compared with Cauchy Integral Method, which is commonly used to obtain complex roots. Furthermore, the relationship between the amplitudes of the different regions is obtained, whereby the whole structure can be analyzed as a single one from now on.

## 1. INTRODUCTION

The computation of the complex resonant frequencies in microwave structures is usually carried out through numerical methods, where the most effective modal methods, such as *mode-matching* or *circuit* techniques, solve an eigenvalue problem numerically to get the solutions [1, 2]. These methods consist of the segmentation of the whole geometry to get simpler regions which can be analyzed easily. Then all the simpler regions are joined together to analyze the whole resonant structure. The problem arises when the structure has many zones, because the eigenvalue problem becomes huge and, as a consequence, the resolution speed and convergence goes down quickly.

In order to reduce the complexity of some geometries, some authors, such as Harrington [3], Collin [4], Zaki and Atia [5], Blackburn [6], and Xi and Tinga [7], combine the regions which can be treated as a single zone, reducing the number of regions of the whole structure. So far, the main drawback of this procedure is the lack of generality, because all the authors propose only specific and simple cases, as 2-3 *slabs* [3, 8] or 2–3 loaded regions [5, 7, 9]. When the number of regions increases, numerical methods replace analytical solutions [6, 10].

In this paper, we propose a general analysis of the  $N$  *slabs* cylindrical structure, getting an analytical solution of the electromagnetic fields, as well as the characteristic equations for TE and TM modes, whose roots provide the complex resonant frequencies, wavenumbers and/or propagation constants.

To solve the characteristic equations, we have developed an algorithm, based on Chebyshev's root finder [11], which provides solutions without initial seed (necessary in most of numerical methods). Furthermore, the accuracy and computational speed are really good compared with other root finders from the literature.

With this analysis, a generic region with  $N$  *slabs* can be treated as a single zone, simplifying significantly the complexity of the modeling of this type of structures.

---

Received 9 February 2017, Accepted 15 June 2017, Scheduled 20 June 2017

<sup>\*</sup> Corresponding author: David Marques-Villarroya (damarvi3@itaca.upv.es).

The authors are with the Instituto ITACA, Universitat Politècnica de València, Camino de Vera, s/n, 46022-Valencia, Spain.

## 2. ELECTROMAGNETIC THEORY

The analyzed structure consists of a cylindrical multilayer cavity with  $N$  slabs of different dielectric properties (see Fig. 1). This structure can be solved analytically; in fact, the simplest cases with 2 and 3 slabs are treated in [3] and [8] respectively. In this work, we are going to generalize the analytical expressions of this type of configuration (with  $N$  slabs).

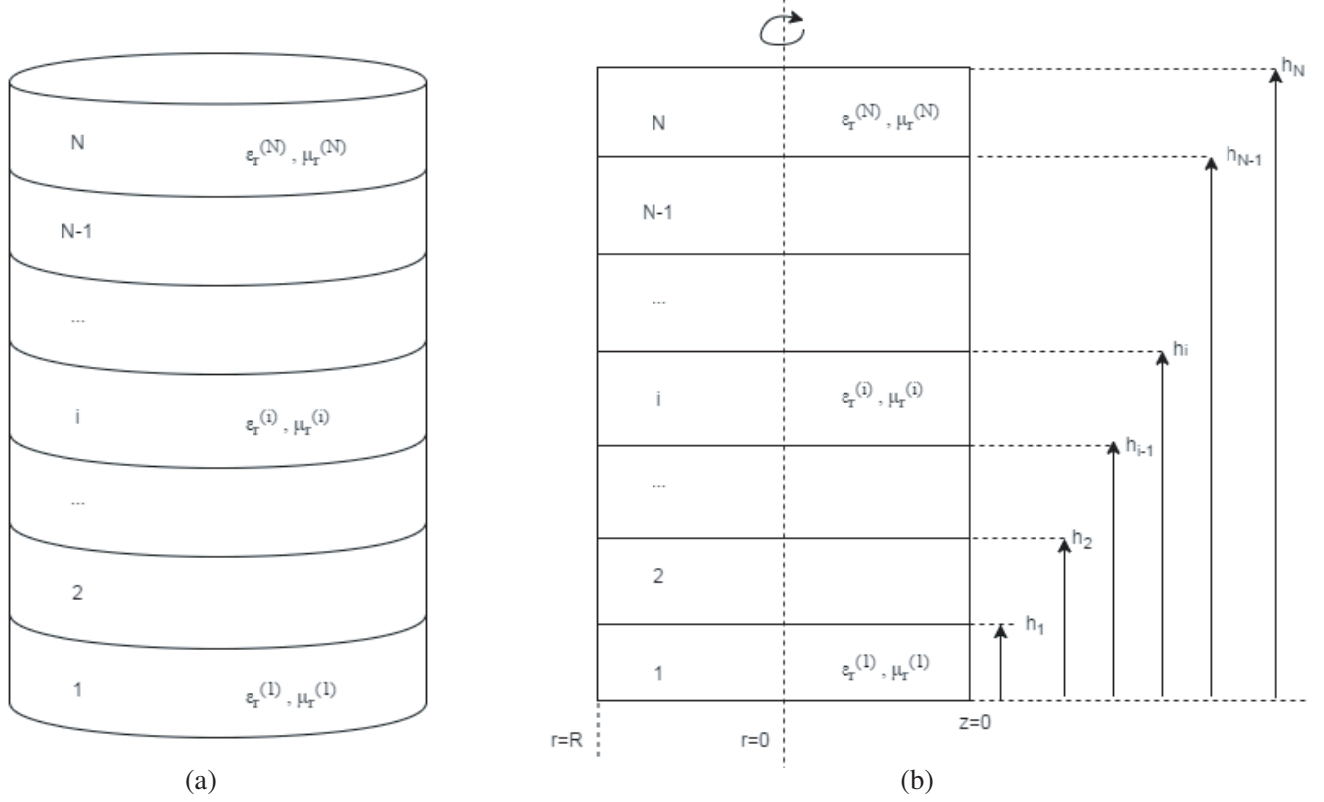


**Figure 1.** Cylindrical Cavity with  $N$  slabs. (a) 3D view. (b) Cross section.

To solve the electromagnetic fields, we have to enforce the following boundary conditions (assuming perfect conductors on the walls of the cavity) [12]:

$$E_t^{(i)} \Big|_{r=R} = 0, \quad 1 \leq i \leq N \quad (1)$$

$$E_t^{(1)} \Big|_{z=0} = 0 \quad (2)$$

$$\begin{cases} E_t^{(i)} \Big|_{z=h_{i-1}} = E_t^{(i-1)} \Big|_{z=h_{i-1}} \\ H_t^{(i)} \Big|_{z=h_{i-1}} = H_t^{(i-1)} \Big|_{z=h_{i-1}} \end{cases}, \quad 2 \leq i \leq N-1 \quad (3)$$

$$E_t^{(N)} \Big|_{z=h_N} = 0 \quad (4)$$

The modes inside the cavity can be separated in transversal electric (TE) and magnetic (TM) modes, because of the geometry. Then, we can analyze both cases individually.

## 2.1. TM Modes

The expressions of the electric and magnetic fields inside the circular cavities can be found in [13]. The expressions for each  $i^{th}$  slab are shown below.

$$E_z^{(i)} = \sum_{mn} \begin{pmatrix} \sin(m\varphi) \\ \cos(m\varphi) \end{pmatrix}^T \begin{pmatrix} A_i^s \\ A_i^c \end{pmatrix} J_m(k_{cn}r) \left( A_i^+ e^{-\gamma_n^{(i)}z} + A_i^- e^{\gamma_n^{(i)}z} \right) \quad (5a)$$

$$E_r^{(i)} = \sum_{mn} \frac{-\gamma_n^{(i)}}{k_{cn}} \begin{pmatrix} \sin(m\varphi) \\ \cos(m\varphi) \end{pmatrix}^T \begin{pmatrix} A_i^s \\ A_i^c \end{pmatrix} J'_m(k_{cn}r) \left( A_i^+ e^{-\gamma_n^{(i)}z} - A_i^- e^{\gamma_n^{(i)}z} \right) \quad (5b)$$

$$E_\varphi^{(i)} = \sum_{mn} \frac{-\gamma_n^{(i)}}{k_{cn}^2} \frac{m}{r} \begin{pmatrix} \cos(m\varphi) \\ -\sin(m\varphi) \end{pmatrix}^T \begin{pmatrix} A_i^s \\ A_i^c \end{pmatrix} J_m(k_{cn}r) \left( A_i^+ e^{-\gamma_n^{(i)}z} - A_i^- e^{\gamma_n^{(i)}z} \right) \quad (5c)$$

$$H_z^{(i)} = 0 \quad (5d)$$

$$H_r^{(i)} = \sum_{mn} \frac{-j\omega\varepsilon_i}{k_{cn}^2} \frac{m}{r} \begin{pmatrix} \cos(m\varphi) \\ -\sin(m\varphi) \end{pmatrix}^T \begin{pmatrix} A_i^s \\ A_i^c \end{pmatrix} J_m(k_{cn}r) \left( A_i^+ e^{-\gamma_n^{(i)}z} + A_i^- e^{\gamma_n^{(i)}z} \right) \quad (5e)$$

$$H_\varphi^{(i)} = \sum_{mn} \frac{-j\omega\varepsilon_i}{k_{cn}} \begin{pmatrix} \sin(m\varphi) \\ \cos(m\varphi) \end{pmatrix}^T \begin{pmatrix} A_i^s \\ A_i^c \end{pmatrix} J'_m(k_{cn}r) \left( A_i^+ e^{-\gamma_n^{(i)}z} + A_i^- e^{\gamma_n^{(i)}z} \right) \quad (5f)$$

where,  $A_i^{s/c}$  are the amplitudes associated with the trigonometric functions;  $A_i^+ A_i^-$  are the incoming and outgoing coefficients, respectively;  $J_m, J'_m$  are the Bessel function of first kind and order  $m$  and its derivative;  $\varepsilon_i, \mu_i$  are the permittivity and the permeability;  $\gamma_n^{(i)}$  is the propagation constant in each slab and  $k_{cn}$  is the wave number, which is the same for all the slabs because of the geometry. The propagation constant and the wavenumber are related as follow:

$$k_{cn}^2 = \left( \gamma_n^{(i)} \right)^2 - \varepsilon_r^{(i)} \mu_r^{(i)} k_0^2 \quad (6)$$

Enforcing Eq. (1) we get  $k_{cn} = \frac{\chi_{mn}}{R}$ , where  $\chi_{mn}$  is the  $n^{th}$  zero of the Bessel function first kind of order  $m$ .

Applying boundary conditions on the bottom ( $z = 0$ ) of the cavity in Eq. (2), we achieve the relationship between the progressive and regressive amplitudes of the region 1:  $A_1^+ = A_1^-$ .

In the intermediates slabs, we have to enforce the continuity of the electric and magnetic fields over every separation interface  $h_i$  in Eq. (3). Then, we achieve the relationship between the amplitudes of the region  $i$  and the previous region,  $i - 1$ .

$$\begin{cases} A_i^+ = K_{ni}^{++} A_{i-1}^+ - K_{ni}^{+-} A_{i-1}^- \\ A_i^- = K_{ni}^{-+} A_{i-1}^+ - K_{ni}^{--} A_{i-1}^- \end{cases} \quad (7)$$

where,

$$K_{ni}^{++} = e^{\gamma_n^{(i)} h_{i-1}} e^{-\gamma_n^{(i-1)} h_{i-1}} \Gamma_i^+ / 2 \quad (8a)$$

$$K_{ni}^{+-} = e^{\gamma_n^{(i)} h_{i-1}} e^{\gamma_n^{(i-1)} h_{i-1}} \Gamma_i^- / 2 \quad (8b)$$

$$K_{ni}^{-+} = -e^{-\gamma_n^{(i)} h_{i-1}} e^{-\gamma_n^{(i-1)} h_{i-1}} \Gamma_i^- / 2 \quad (8c)$$

$$K_{ni}^{--} = -e^{-\gamma_n^{(i)} h_{i-1}} e^{\gamma_n^{(i-1)} h_{i-1}} \Gamma_i^+ / 2 \quad (8d)$$

$$\Gamma_i^+ = \left( \frac{\gamma_n^{(i-1)}}{\gamma_n^{(i)}} + \frac{\varepsilon_r^{(i-1)}}{\varepsilon_r^{(i)}} \right) \quad (8e)$$

$$\Gamma_i^- = \left( \frac{\gamma_n^{(i-1)}}{\gamma_n^{(i)}} - \frac{\varepsilon_r^{(i-1)}}{\varepsilon_r^{(i)}} \right) \quad (8f)$$

At this point, we are able to provide a recursive expression which relates the amplitudes of the  $i^{th}$  slab with the amplitudes of the region 1, where we know that progressive and regressive amplitudes are equal ( $A_1^+ = A_1^-$ ).

$$\begin{cases} A_i^+ = M_i^+ A_1^+ \\ A_i^- = M_i^- A_1^+ \end{cases}, \quad i = 2, N \quad (9)$$

where,

$$\begin{cases} M_i^+ = K_{ni}^{++} M_{i-1}^+ - K_{nj}^{+-} M_{i-1}^- \\ M_i^- = K_{ni}^{-+} M_{i-1}^+ - K_{nj}^{--} M_{i-1}^- \end{cases} \quad (10)$$

and

$$M_1^+ = e^{\gamma_n^{(2)} h_1} \left( -\frac{\gamma_n^{(1)}}{\gamma_n^{(2)}} \sinh(\gamma_n^{(1)} h_1) + \frac{\varepsilon_r^{(1)}}{\varepsilon_r^{(2)}} \cosh(\gamma_n^{(1)} h_1) \right) \quad (11a)$$

$$M_1^- = e^{-\gamma_n^{(2)} h_1} \left( \frac{\gamma_n^{(1)}}{\gamma_n^{(2)}} \sinh(\gamma_n^{(1)} h_1) + \frac{\varepsilon_r^{(1)}}{\varepsilon_r^{(2)}} \cosh(\gamma_n^{(1)} h_1) \right) \quad (11b)$$

Finally, applying the last boundary condition in Eq. (4) on the top of the cavity ( $z = h_N$ ), we achieve the relationship between the progressive and regressive amplitudes of the region  $N$ ,  $A_N^- = A_N^+ e^{-2\gamma_n h_N}$ .

Then, making use of Eq. (9), for  $i = N$ , and the last relation obtained, we get a characteristic equation to calculate the complex resonant frequency, wave number or propagation constant.

$$\begin{aligned} & \gamma_n^{(N-1)} \varepsilon_r^{(N)} \left( M_{N-1}^+ e^{-\gamma_n^{(N-1)} h_{N-1}} - M_{N-1}^- e^{\gamma_n^{(N-1)} h_{N-1}} \right) \cosh(\gamma_n^{(N)} (h_{N-1} - h_N)) \\ & + \gamma_n^{(N)} \varepsilon_r^{(N-1)} \left( M_{N-1}^+ e^{-\gamma_n^{(N-1)} h_{N-1}} + M_{N-1}^- e^{\gamma_n^{(N-1)} h_{N-1}} \right) \sinh(\gamma_n^{(N)} (h_{N-1} - h_N)) = 0 \end{aligned} \quad (12)$$

## 2.2. TE Modes

The analysis of the TE modes is similar to TM modes, but changing the expressions of the electromagnetic fields.

The electric and magnetic fields of TE modes in the  $i^{th}$  slab can be expressed as follow [13]:

$$E_z^{(i)} = 0 \quad (13a)$$

$$E_r^{(i)} = \sum_{mn} \frac{j\omega\mu_i m}{k_{cn}^2 r} \begin{pmatrix} \cos(m\varphi) \\ -\sin(m\varphi) \end{pmatrix}^T \begin{pmatrix} A_i^s \\ A_i^c \end{pmatrix} J_m(k_{cn}r) \left( A_i^+ e^{-\gamma_n^{(i)} z} + A_i^- e^{\gamma_n^{(i)} z} \right) \quad (13b)$$

$$E_\varphi^{(i)} = \sum_{mn} \frac{j\omega\mu_i}{k_{cn}} \begin{pmatrix} \sin(m\varphi) \\ \cos(m\varphi) \end{pmatrix}^T \begin{pmatrix} A_i^s \\ A_i^c \end{pmatrix} J'_m(k_{cn}r) \left( A_i^+ e^{-\gamma_n^{(i)} z} + A_i^- e^{\gamma_n^{(i)} z} \right) \quad (13c)$$

$$H_z^{(i)} = \sum_{mn} \begin{pmatrix} \sin(m\varphi) \\ \cos(m\varphi) \end{pmatrix}^T \begin{pmatrix} A_i^s \\ A_i^c \end{pmatrix} J_m(k_{cn}r) \left( A_i^+ e^{-\gamma_n^{(i)} z} + A_i^- e^{\gamma_n^{(i)} z} \right) \quad (13d)$$

$$H_r^{(i)} = \sum_{mn} \frac{-\gamma_n^{(i)}}{k_{cn}} \begin{pmatrix} \sin(m\varphi) \\ \cos(m\varphi) \end{pmatrix}^T \begin{pmatrix} A_i^s \\ A_i^c \end{pmatrix} J'_m(k_{cn}r) \left( A_i^+ e^{-\gamma_n^{(i)} z} - A_i^- e^{\gamma_n^{(i)} z} \right) \quad (13e)$$

$$H_\varphi^{(i)} = \sum_{mn} \frac{-\gamma_n^{(i)} m}{k_{cn}^2 r} \begin{pmatrix} \cos(m\varphi) \\ -\sin(m\varphi) \end{pmatrix}^T \begin{pmatrix} A_i^s \\ A_i^c \end{pmatrix} J_m(k_{cn}r) \left( A_i^+ e^{-\gamma_n^{(i)} z} - A_i^- e^{\gamma_n^{(i)} z} \right) \quad (13f)$$

Applying the boundary condition on the lateral wall of the cavity in Eq. (1),  $k_{cn} = \frac{\chi'_{mn}}{R}$ , where  $\chi'_{mn}$  is the  $n^{th}$  zero of the derivative of the Bessel function of first kind and order  $m$ .

The relationship between the incoming and outgoing coefficients of the region 1 is given by enforcing Eq. (2):  $A_1^+ = -A_1^-$ .

In the intermediates *slabs*, we enforce Eq. (3), getting the relationship between the amplitudes of the region  $i$  and the previous  $i - 1$ .

$$\begin{cases} A_i^+ = K_{ni}^{++} A_{i-1}^+ + K_{ni}^{+-} A_{i-1}^- \\ A_i^- = K_{ni}^{-+} A_{i-1}^+ + K_{ni}^{--} A_{i-1}^- \end{cases} \quad (14)$$

where,

$$K_{ni}^{++} = e^{\gamma_n^{(i)} h_{i-1}} e^{-\gamma_n^{(i-1)} h_{i-1}} \Gamma_i^+ / 2 \quad (15a)$$

$$K_{ni}^{+-} = e^{\gamma_n^{(i)} h_{i-1}} e^{\gamma_n^{(i-1)} h_{i-1}} \Gamma_i^- / 2 \quad (15b)$$

$$K_{ni}^{-+} = e^{-\gamma_n^{(i)} h_{i-1}} e^{-\gamma_n^{(i-1)} h_{i-1}} \Gamma_i^- / 2 \quad (15c)$$

$$K_{ni}^{--} = e^{-\gamma_n^{(i)} h_{i-1}} e^{\gamma_n^{(i-1)} h_{i-1}} \Gamma_i^+ / 2 \quad (15d)$$

$$\Gamma_i^+ = \left( \frac{\mu_r^{(i-1)}}{\mu_r^{(i)}} + \frac{\gamma_n^{(i-1)}}{\gamma_n^{(i)}} \right) \quad (15e)$$

$$\Gamma_i^- = \left( \frac{\mu_r^{(i-1)}}{\mu_r^{(i)}} - \frac{\gamma_n^{(i-1)}}{\gamma_n^{(i)}} \right) \quad (15f)$$

The recursive expression which relates the amplitudes of the  $i^{th}$  slab with the amplitudes of the region 1, for TE modes, is:

$$\begin{cases} A_i^+ = M_i^+ A_1^+ \\ A_i^- = M_j^- A_1^+ \end{cases}, \quad i = 2, N \quad (16)$$

where,

$$\begin{cases} M_i^+ = K_{ni}^{++} M_{i-1}^+ + K_{ni}^{+-} M_{i-1}^- \\ M_i^- = K_{ni}^{-+} M_{i-1}^+ + K_{ni}^{--} M_{i-1}^- \end{cases} \quad (17)$$

and

$$M_1^+ = e^{\gamma_n^{(2)} h_1} \left( \frac{\mu_r^{(1)}}{\mu_r^{(2)}} \left( -\sinh \left( \gamma_n^{(1)} h_1 \right) \right) + \frac{\gamma_n^{(1)}}{\gamma_n^{(2)}} \cosh \left( \gamma_n^{(1)} h_1 \right) \right) \quad (18a)$$

$$M_1^- = -e^{-\gamma_n^{(2)} h_1} \left( \frac{\mu_r^{(1)}}{\mu_r^{(2)}} \sinh \left( \gamma_n^{(1)} h_1 \right) + \frac{\gamma_n^{(1)}}{\gamma_n^{(2)}} \cosh \left( \gamma_n^{(1)} h_1 \right) \right) \quad (18b)$$

The last boundary condition, on the top of the cavity in Eq. (4), provides the relation between the progressive and regressive amplitudes of the region  $N$ :  $A_N^- = -A_N^+ e^{-2\gamma_n^{(N)} h_N}$ .

Then, using Eq. (16), for  $i = N$ , and the last relation obtained, we achieve the characteristic equation for TE modes.

$$\begin{aligned} & \gamma_n^{(N-1)} \mu_r^{(N)} \left( M_{N-1}^+ e^{-\gamma_n^{(N-1)} h_{i-1}} - M_{N-1}^- e^{\gamma_n^{(N-1)} h_{N-1}} \right) \sinh \left( \gamma_n^{(N)} (h_{N-1} - h_N) \right) \\ & + \gamma_n^{(N)} \mu_r^{(N-1)} \left( M_{N-1}^+ e^{-\gamma_n^{(N-1)} h_{N-1}} + M_{N-1}^- e^{\gamma_n^{(N-1)} h_{N-1}} \right) \cosh \left( \gamma_n^{(N)} (h_{N-1} - h_N) \right) = 0 \end{aligned} \quad (19)$$

In this work, we are going to calculate the complex resonant frequency making use of the characteristic equations, but as we mentioned above, we can obtain the propagation constants or the wave numbers too.

### 3. CHEBYSHEV'S ROOT FINDER

There are many root finders in the literature to solve the characteristic equations described above. However, usually, most of them need an initial seed, and they only provide a single root.

In our case, we are interested in the achievement of multiple roots, because they provide the resonant frequency for every single mode. Furthermore, we know previously that those roots are on the real axis if the dielectrics are ideal (without losses); otherwise, when the dielectrics have losses, the imaginary part of the roots is going to be much smaller than the real part.

With this previous knowledge, one of the most suitable root finder algorithms is the Chebyshev method proposed in [11]. We chose this one because in [14] the method is extended to achieve slightly complex roots too, whereby fits perfectly with our requirements.

The method basically consists of the approximation of a continuous function  $f(x)$  by Chebyshev's polynomial over a closed interval  $[a, b]$ . Then, applying the method proposed in [11] and [14], the zeros of the function  $f(x)$  in the interval  $[a, b]$  are calculated.

Applying an iterative algorithm, where the search interval  $[a, b]$  moves along the  $x$  axis, we are able to get as many roots as one desires. We just need an initial point to start the search ( $x_0$ ) and an incremental value to fix the interval ( $\Delta x = b - a$ ). The algorithm developed to find multiple real or slightly complex roots ( $N$ ) of a general function  $f(x)$  is shown in Fig. 2.

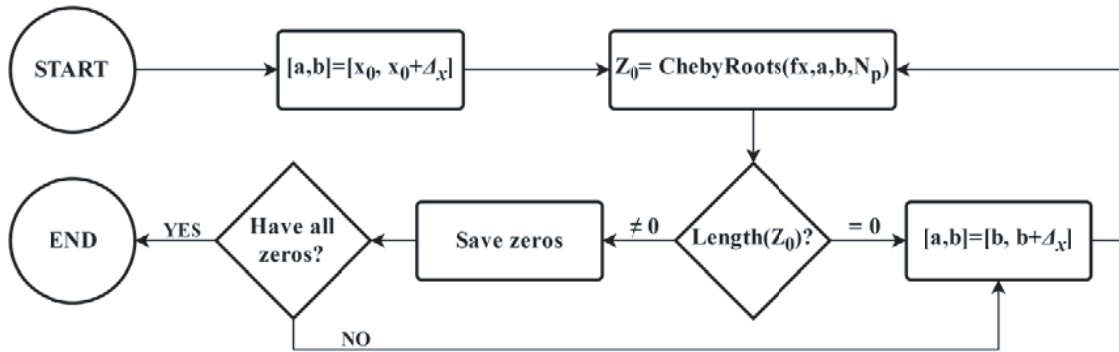


**Figure 2.** Algorithm to find multiple roots of a generic function making use of the Chebyshev's root-finder. The subroutine ChebyRoots gets all the roots of  $f(x)$  in the interval  $[a, b]$ .

In our case,  $f(x)$  is the TM or TE characteristic equation obtained before, where the unknown variable is the free-space wavenumber constant ( $k_0$ ), which is directly related with the complex resonant frequency ( $\Omega_r$ ):

$$k_0 = 2\pi\Omega_r\sqrt{\varepsilon_0\mu_0}; \quad \Omega_r = f_r \left( 1 + \frac{j}{2Q} \right) \quad (20)$$

Those equations, (12) and (19), are continuous, and they have been formulated to avoid discontinuities and possible poles which could endanger the convergence of the Chebyshev's method [11].

We have fixed the initial point  $x_0 = 0$  and the incremental value  $\Delta x = 5$ , because of the order of magnitude of the free-space wavenumber. Another parameter that must be fixed is the order of the Chebyshev's polynomial ( $N_p$ ), we have chosen  $N_p = 15$ , because it is high enough to model correctly the function  $f(x)$  over the defined interval. These parameters have been obtained empirically. With the proposed values the convergence and a good behavior of the method for the resolution of the characteristic equations are ensured.

This root finder fits the specifications of the problem perfectly, though there are others that can also be employed to solve the characteristic equations successfully, such as those using the Cauchy's argument principle [15]. The main advantage of the root finder employed in this work is the low computational cost and high accuracy that it provides. On the other hand, the Cauchy Integral methods ensure the acquisition of the entire set of complex roots, while with Chebyshev's method, parameters must be chosen carefully to ensure that all the roots are obtained.

#### 4. NUMERICAL RESULTS

Throughout this section, we are going to study 3 different configurations with different numbers of *slabs*, heights ( $H$ ), permittivities ( $\varepsilon_r$ ) and permeabilities ( $\mu_r$ ).

(i) Configuration 1 (C1): 3 slabs.

$$\begin{aligned} H &= [12, 20, 45] \text{ mm. } R = 25 \text{ mm.} \\ \varepsilon_r &= [2.5 - 0.0012j, 3.18 - 0.0002j, 2.89 - 0.0024j] \\ \mu_r &= [1, 1, 1] \end{aligned}$$

(ii) Configuration 2 (C2): 5 slabs.

$$\begin{aligned} H &= [10, 17, 28, 36, 58] \text{ mm. } R = 16.5 \text{ mm.} \\ \varepsilon_r &= [10 - 0.02j, 2.1 - 0.0011j, 5.2 - 0.0052j, 2.1 - 0.0011j, 1 - 0.0001j] \\ \mu_r &= [1, 0.89 - 0.001j, 1, 0.89 - 0.001j, 1] \end{aligned}$$

(iii) Configuration 3 (C3): 7 slabs.

$$\begin{aligned} H &= [8, 15, 22, 38, 42, 68, 87] \text{ mm. } R = 42 \text{ mm.} \\ \varepsilon_r &= [5.1 - 0.001j, 2.2 - 0.025j, 1, 3.64 - 0.0364j, 6.87 - 0.12j, 4.67 - 0.052j, 1] \\ \mu_r &= [0.65 - 0.005j, 0.72 - 0.0072j, 1, 0.57 - 0.041j, 0.98 - 0.000098j, 0.77 - 0.064j, 1] \end{aligned}$$

All the results presented in this paper are performed using MATLAB on a Pentium (R) Dual-Core 2.94 GHz PC.

Firstly, some resonant frequencies ( $f_r$ ) and quality factors ( $Q$ ) of 3 different configurations are calculated, employing the characteristic Equations (12) and (19), and making use of the Chebyshev's root finder algorithm explained above. The results are compared with a numerical method developed in [16], which consist of a *full-wave circuit* technique for the analysis of circular cavities. The relative differences between both methods are negligible (less than 0.5% in all the cases).

**Table 1.** Comparison between characteristic equation method and numerical technique [16] in the computation of the resonant frequency and quality factor of 3 different configurations and for some different modes.

Config.	Mode	$f_r$ -Ch. Eq. (GHz)	$Q$ -Ch. Eq.	$f_r$ -Num. (GHz)	$Q$ -Num.	$\Delta f_r$ (%)	$\Delta Q$ (%)
C1	TM <sub>111</sub>	4.83531050	1725.48	4.83531123	1725.46	$1.5 \cdot 10^{-5}$	0.0011
	TE <sub>211</sub>	5.79753392	1476.38	5.79753421	1476.32	$0.5 \cdot 10^{-5}$	0.0041
C2	TM <sub>210</sub>	5.18511106	510.11	5.18511364	510.05	$4.98 \cdot 10^{-5}$	0.012
	TE <sub>011</sub>	4.90015355	473.47	4.90015124	473.41	$4.7 \cdot 10^{-5}$	0.013
C3	TM <sub>012</sub>	2.97507770	33.59	2.97507748	33.63	$0.74 \cdot 10^{-5}$	0.12
	TE <sub>111</sub>	1.51489037	16.28	1.51489369	16.22	$22 \cdot 10^{-5}$	0.37

It is important to remark that the roots of the characteristic equations are the free-space wavenumbers as mentioned above, and then the resonant frequency and the quality factor are obtained applying the relation (20). Note that even for the lowest quality factor (inversely proportional to imaginary part of the complex resonant frequency), the accuracy is still good. This is because the free-space wavenumber (unknown variable of the characteristic equations) remains slightly complex even for low  $Q$ , whereby Chebyshev's root finder works correctly. When the imaginary part becomes comparable with the real part, the Chebyshev's root finder does not work properly, and other root finder should be employed, though that is not our case.

Note that for *full-wave* circuit method, is not possible the application of Chebyshev's root finder, since it solves an eigenvalue problem [16], which has implicit the absolute value function ( $|\det(X)| = 0$ ) that produces multiple discontinuities.

In Table 2, the accuracy of the roots calculated by Chebyshev's root finder and Cauchy integral method is validated. The results have a really good agreement. However, the computational speed is much worst employing Cauchy method, as one can see in Fig. 3.

**Table 2.** Accuracy of the Chebyshev's root finder and Cauchy Integral method. The zeros are for the  $TM_{111}$  mode.

Config.	$k_0^{CHEBY}$	$k_0^{CAUCHY}$
C1	$101.34 + 0.029j$	$101.33 + 0.021j$
C2	$131.12 + 0.073j$	$131.17 + 0.071j$
C3	$72.47 + 1.071j$	$72.366 + 1.209j$

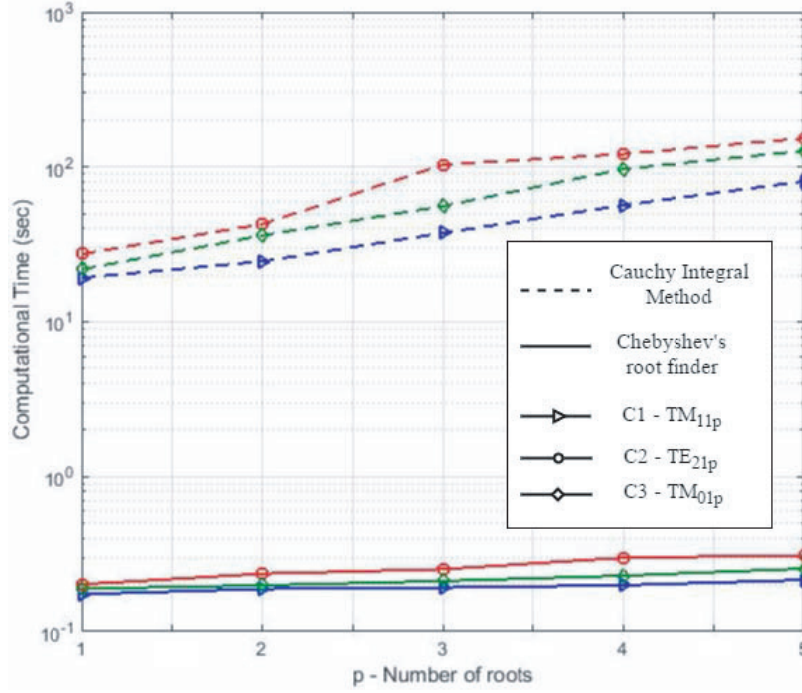


**Figure 3.** Comparison of the computational time spent with Chebyshev's root finder and Cauchy Integral method to obtain  $p$  roots of the characteristic equations.

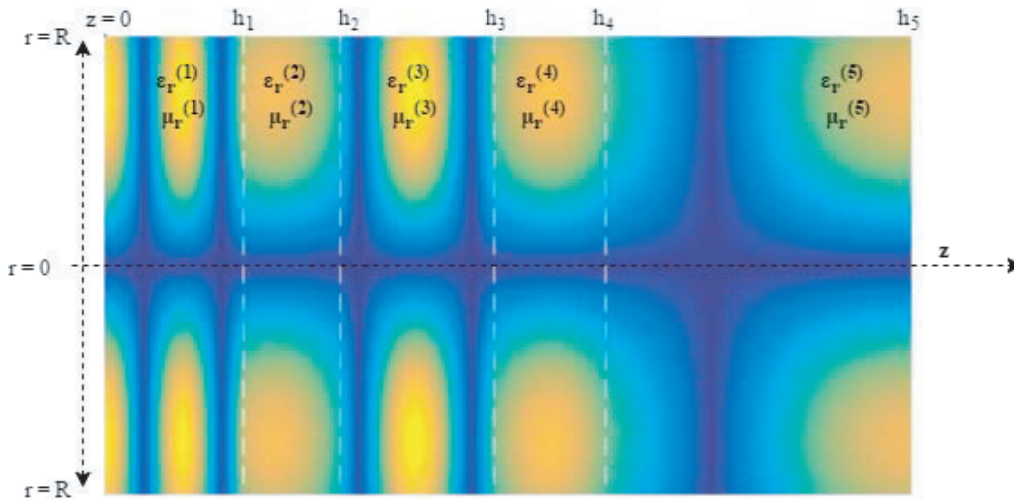


**Figure 4.**  $|\vec{H}|$  of the  $TM_{015}$  resonant mode of the configuration C2.

Finally, Fig. 4 shows the magnetic field distribution of the  $TM_{015}$  resonant mode of the configuration C2, where one can see the field continuity in the azimuthal planes  $z = h_i$ , validating the correct application of the boundary conditions. It is important to remark that, for the plotting of the fields, we have only made use of the amplitudes of the first *slab*, following the relationship obtained in Equation (9). Therefore, we have analyzed the whole structure as a single one, with the amplitudes of the region 1 uniquely. As expected, in the regions with higher dielectric constant (1 and 3), the field intensity is stronger than the others (2-4-5).

## 5. CONCLUSIONS

In this paper, an efficient analysis to obtain the complex resonant frequencies of the multilayer circular cavity has been performed. We have deduced a generic and explicit characteristic equation for both TM and TE resonant modes, making use of some recursive expressions, which can be employed to analyze this type of structures analytically instead of the classical numerical methods such as the mentioned *full-wave* circuit analysis, improving significantly the computational speed.

To solve the characteristic equations, an efficient algorithm based on Chebyshev's root finder has been developed, obtaining better computational results than classical root finders based of Cauchy's argument principle.

Finally, with this study, as we mentioned through the paper, a multilayer geometry with  $N$  circular *slabs* of different dielectrics can be treated as a single region, which could be really useful for futures *mode-matching* analysis.

## ACKNOWLEDGMENT

This work has been financially supported by "Programa de Ayudas de Investigación y Desarrollo (PAID) de la Universitat Politècnica de València", "Programa de Apoyo a la investigación y Desarrollo (PAID-00-15) de la Universitat Politècnica de València", and by "Conselleria de Educación, Investigación, Cultura y Deporte. Generalitat Valenciana (BEST/2016/012)".

Results are obtained under the project SEDMICRON — TEC2015-70272-R (MINECO/FEDER), financed by Ministerio de Economía y Competitividad (MINECO) -Spanish Government- and by European Regional Development Funds (ERDF) of European Union.

## REFERENCES

1. Conciauro, G., M. Guglielmi, and R. Sorrentino, *Advanced Modal Analysis*, Wiley, New York, NY, USA, 1999.
2. Penaranda-Foix, F. L. and J. M. Catala-Civera, "Circuitual analysis of cylindrical structures applied to the electromagnetic resolution of resonant cavities," *Passive Microwave Components and Antennas*, Ch. 7, InTech, Vukovar, Croatia, Apr. 2010.
3. Harrington, R. F., *Time-Harmonic Electromagnetic Fields*, New York, 1961, ISBN 047120806X.
4. Collin, R. E., *Foundations for Microwave Engineering*, McGraw-Hill, New York, 1966
5. Zaki, K. A. and A. E. Atia, "Modes in dielectric-loaded waveguides and resonators," *IEEE Transactions on Microwave Theory and Techniques*, Vol. 31, No. 12, 1039–1045, Dec. 1983.
6. Blackburn, J., "Solving the double eigenvalue problem: A study of mode matching in arbitrary-layer dielectric resonators," *IEE Proceedings — Microwaves, Antennas and Propagation*, Vol. 153, No. 5, 447–455, Oct. 2006.
7. Xi, W. and W. R. Tinga, "Field analysis of new coaxial dielectrometer," *IEEE Transactions on Microwave Theory and Techniques*, Vol. 40, No. 10, 1927–1934, Oct. 1992.
8. Chen, S. W. and K. A. Zaki, "A novel coupled method for dual-mode dielectric resonators and waveguide filters," *IEEE Transactions on Microwave Theory and Techniques*, Vol. 38, No. 12, 1885–1893, Dec. 1990.

9. Penaranda-Foix, F. L., J. M. Catala-Civera, A. J. Canós, and B. Garcia-Banos, “Finding resonant frequencies for high loss dielectrics in cylindrical cavities,” *Int. J. RF and Microwave Comp. Aid. Eng.*, Vol. 25, 530–535, 2015.
10. Wang, C. and K. A. Zaki, “Generalized multilayer anisotropic dielectric resonators,” *IEEE Transactions on Microwave Theory and Techniques*, Vol. 48, No. 1, 60–66, Jan. 2000.
11. Boyd, J. P., “Computing zeros on a real interval through Chebyshev expansion and polynomial rootfinding,” *SIAM J. Numer. Anal.*, Vol. 40, 1666–1682, 2002.
12. Collin, R. E., *Field Theory of Guided Waves*, IEEE Press, 1991, ISBN 978-0879422370.
13. Balanis, C. A., *Advanced Engineering Electromagnetics*, John Wiley & Sons, 1989.
14. Boyd, J. P., “Finding the zeros of a univariate equation: Proxy rootfinders, Chebyshev interpolation, and the companion matrix,” *SIAM Review*, Vol. 55, No. 2, 375–396, 2013.
15. Penaranda-Foix, F. L., M. Contelles-Cervera, P. J. Plaza-Gonzalez, and J. M. Catala-Civera, “Solving the cut-off wave numbers in partially filled rectangular waveguides with ferrite by the Cauchy integral method,” *2005 IEEE Antennas and Propagation Society International Symposium*, Vol. 2B, 626–629, 2005.
16. Marqués-Villarroya, D., F. L. Peñaranda-Foix, B. García-Baños, J. M. Catalá-Civera, and J. D. Gutiérrez-Cano, “Enhanced full-wave circuit analysis for modeling of a split cylinder resonator,” *IEEE Transactions on Microwave Theory and Techniques*, Vol. 65, No. 4, 1191–1202, Apr. 2017.